# Resonant lidar detection of Ca and Ca+ in the upper atmosphere

Claire Granier, Jean-Pierre Jégou, Gérard Mégie

RESONANT LIDAR DETECTION OF CA AND CA$^+$ IN THE UPPER ATMOSPHERE

C. Granier, J.P. Jégou and G. Mégie

Service d'Aéronomie du CNRS, BP 3 - 91370 - Verrières le Buisson
France

Abstract. Resonant lidar detection of neutral (Ca-423 nm) and ionized ( Ca$^+$ - 393 nm) calcium altitude distributions has been performed during nighttime at the Observatoire de Haute-Provence. The emitter is composed of two Nd-Yag pumped dye lasers, the 393 nm emission being obtained by three waves mixing in a non-linear crystal. The first detection of Ca has been carried out in December, 1982 and has shown that the integrated abundance of the atomic form is low, with a value of about $1.5 \times 10^7$ cm$^{-2}$, further confirmed by measurement performed in July, 1983. During this same month, the detection of Ca$^+$ has been achieved, proving the lidar ability to follow rapid evolutions of Ca$^+$ layers, which appear between 85 and 115 km altitudes.

Introduction

Fifteen years ago, the scientific interest in upper atmospheric sodium and the appearance of newly developed flashlamp pumped dye lasers both stimulated atmospheric lidar developments. Sodium lidar observations are currently carried out with a continuous increase both in spatial and temporal resolutions (Shelton et al., 1980; Clemesha et al., 1982; Granier and Mégie, 1982). Moreover, the lidar detections of atomic potassium and lithium have been performed and have brought some consequent insight into the chemical and dynamical behavior of the metallic elements in the earth upper atmosphere. (Mégie et al., 1978; Jégou et al., 1980). In these experiments the sensitivity limit of resonant scattering lidar measurements has been improved to less than 1 atom cm$^{-3}$. However, while the detection of the only atomic form of these metallic elements is yet available, the modeling of their behavior requires to take into account atomic, ionic and molecular forms (Richter et al., 1979, Jégou et al., 1985). Consequently and in order to get unique informations on the atom-ion relations which could serve to validate the results of model simulations, resonant lidar detection of both neutral (Ca) and ionic (Ca$^+$) calcium has been performed at the Observatoire de Haute Provence (44°N, 6°E). Such a possibility of measuring the two forms exists for calcium as the Ca and Ca$^+$ resonance wavelengths are in the visible region of the spectrum. The interest in improving the set of data by the observations of a non-alkali metal is also evident.

The CaI resonance line at 422.673 nm corresponds to $^1S_0 - ^1P_1$ transition and does not present fine or hyperfine (nuclear spin I = 0) structure. The value of the oscillator strength f and of the peak cross section $\sigma_p$ is subsequently high and the effective linewidth is only limited by the Doppler broadened linewidth $\Delta\lambda_D$ (see Table 1). The CaII resonant absorption, like the alkali atom absorptions, presents a fine structure with two lines, denoted H and K ; the stronger line (K-393.366 nm), chosen for the lidar experiments, corresponds to the absorption from the $^2S_{1/2}$ level up to the $^2P_{3/2}$ level. Complete spectroscopic data for the two transitions are quoted in Table 1. These data are used to calculate the effective cross section (Jégou et al., 1980), which depends on the laser linewidth and allows the calculation of number densities from lidar scattered signals.

Taking into account the high value of the scattering cross-section of the CaI resonance line, the lidar detection of the calcium atom should be relatively easy as its relative abundance is comparable to the sodium one in the meteoritic composition. However, and although lidar detection had not yet been tried, Gadsden (1969) and Broadfoot and Johanson (1976) have tentatively looked for the CaI emission by photometric observations without any success. On the other hand, such observations of the CaII emission have been achieved by different authors (e.g. Broadfoot, 1967; Tepley et al., 1981), while Ca$^+$ measurements by rocket borne mass spectrometer are currently pursued (see for instance Aikin et al., 1977) showing an abundance of the same order of magnitude as the Na$^+$ one. The question of the atomic calcium abundance is thus unresolved at the present time and the lidar observations reported here will give a new insight into this problem.

In this paper only the original experimental set-up and the first results are presented ; a more detailed discussion on their implications in terms of metallic species modeling will be reported in a further publication.

Resonant lidar set-up

Two laser transmitters at the Lidar station at the Observatoire de Haute Provence (OHP) have been adapted to the observation by resonant ex-

TABLE 1. Spectral features of Ca I and CaII resonant excitations. $\lambda_0$ represents the peak wavelength, $f_0$ the oscillator strength, $\Delta\lambda_D$ the Doppler broadening and $\sigma_p$ the peak cross section.

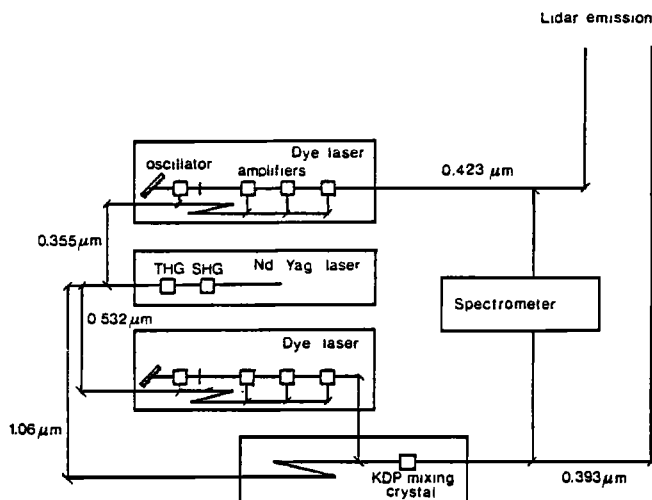| | Ca I | Ca II |
|---|---|---|
| $\lambda_0$ (nm) | 422.673 | 393.366 |
| $f_0$ | 1.75 | 0.69 |
| $\Delta\lambda_D$ (200K) | 0.68 pm | 0.63 pm |
| $\sigma_p$ (cm$^{-2}$) | $3.851 \times 10^{-11}$ | $1.413 \times 10^{-11}$ |

Lidar emission



Fig. 1. Schematic configuration of the Yag-Dye system used to generate the 423 nm and 393 nm wavelengths for resonant excitations of Ca and Ca$^+$.

citation of the two calcium species Ca and Ca$^+$ , layering in the upper atmosphere in the 80-120 km altitude range. The first one, which gives the 423 nm wavelength of atomic calcium resonant excitation, is composed of a dye-laser pumped by the 3rd harmonic of a Nd$^{3+}$-YAG ; the second one combines the red emission of a second dye-laser at 624 nm and the fundamental infrared emission of the Nd$^{3+}$-YAG laser (1064 nm) to give, by frequency mixing in a non-linear KDP crystal, the 393 nm-wavelength of ionic calcium resonant excitation. Beside the possibility of presenting a closed coupling configuration for the two wavelengths emission, as shown in Figure 1, the advantage of the 393 nm frequency mixing generation, as compared with a direct pumping at 355 nm, resides in the use of a rhodamine dye, the pumping efficiency of which is high, and in the fact that the life time of 532 nm pumped dyes is much longer than for any other dye pumped at 355 nm.

The two dye lasers are Jobin-Yvon HPHR lasers (Bos, 1981) which have been modified for this experiment. In both oscillator cavities the spectral tuning and narrowing are achieved by a unique diffraction grating of high groove density used in the Littrow configuration ; one preamplifier and two amplifiers raise the energy to a few tens mJ. Stilbene 420 from Exciton, in a 60 % éthanol - 40 % méthanol solvent are used to generate the 423 nm wavelength with a 1.7 x 10$^{-3}$ mol/l concentration in the resonator and with a 6.7 x 10$^{-4}$ mol/l in the amplifiers (Bucchia et al., 1983). The final characteristics of these two lasers are presented in Table 2. Central wavelengths and spectral profiles of the emissions are controlled in a 1.5 m Czerny-Turner spectrometer (Jobin-Yvon THR) and in a multibeam -Fizeau interferometer with a resolution of 0.5 pm (Cahen et al., 1980). The reference wavelength is given by an hollow cathode lamp.

The receiver is composed of a 80 cm diameter Cassegrain Coudé telescope opened at f/3 and directed to the zenith, a collimator, a dichroïc

thin plate, two interference filters and two photomultiplier tubes cooled by water cooling Peltier effect systems and operated in the photon-counting mode (filter transmissions are quoted in Table 2). The signal is gated every 4 µs , processed in real-time with a LSI 11/23 computer, and the resulting data are stored on floppy disks. The time needed to obtain a signal to noise ratio greater than 20 is comprised between 3 mn and 4 hours, depending upon the species concentrations.

## Results and Discussion

### A.    Ca detection

The first nighttime detection of the calcium atoms was performed during the night of December 21/22, 1982, while the detection of the calcium ion was made during the following summer, in July 1983. The range corrected signal at the peak of the calcium layer observed on December 21/22 is equivalent to the Rayleigh backscattered signal at 64 km. This leads, using an atmospheric model for the atmospheric total density (U.S. Standard, 1976), to a calcium total content of 1.2 x 10$^7$ atoms cm$^{-2}$ and to an average number density of 7 atoms cm$^{-3}$ for a 8 km layer width (peak concentration of 15 atoms cm$^{-3}$) .

Beside the spectrometric control of the wavelength tuning with a 0.5 pm accuracy, a complementary test can be achieved by scanning the laser emission and looking at the variation of the resonantly scattered signal. No significant increase ( < 20 % ) of the calcium abundance which could be related to a detuning of the excitation wavelength position has been detected. Thus, the low value of the calcium abundance appears as a reality. The main errors reside in the evaluation of the effective cross section and in the statistical fluctuations of the signal (Jégou et al., 1980) which can be evaluated to ± 20%.

The calcium layer detected on December 21/22, 1982, shown in Figure 2a, presents a peak at 93 km and its altitude width is 8 km. Whereas these altitude characteristics are comparable with those already observed for the alkali layers, the low value of the Ca total abundance should be emphasized as it is :

- more than a hundred times lower than the sodium abundance, despite a similar abundance of the two elements in the meteoritic source (Anders and Ebihara, 1982).

TABLE 2 . Characteristics of the Lidar systems.

| Transmitter | Ca | Ca$^+$ |
| --- | --- | --- |
| Wavelength | 422.6 nm | 393.4 nm |
| Linewidth | 25 mJ | 20 mJ |
| Beam divergence | 8 x 10$^{-4}$ rad | 10$^{-3}$ rad |
| Repetition rate | 10Hz | 10 Hz |
| Receiver | | |
| Telescope diameter | 0.80 m | 0.80 m |
| Filter bandwidth | 1 nm | 1.3 nm |
| Filter transmission | 18 % | 9 % |
| Sampling gate | 4 µs | 4 µs |

- of the same magnitude or slightly lower than the Ca$^+$ total abundance measured in the same altitude range by mass spectrometry (and by lidar as reported in the next section) whereas

Altitude km



12-22-1982
4:40 - 6 20

Ca number density cm$^{-3}$

Altitude km
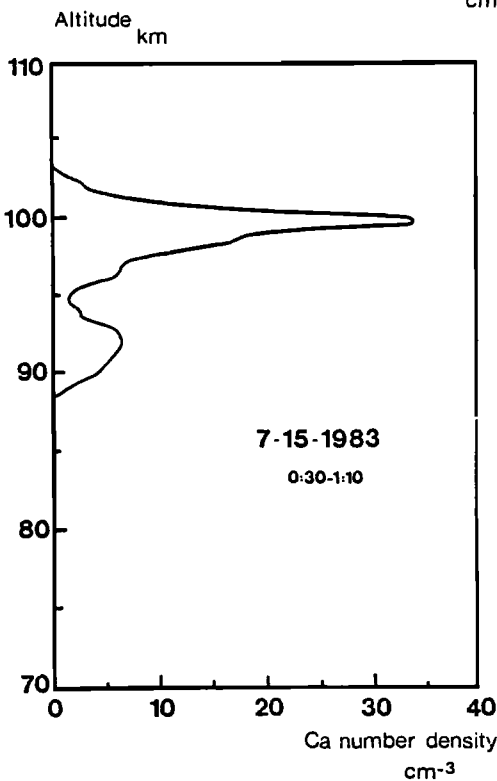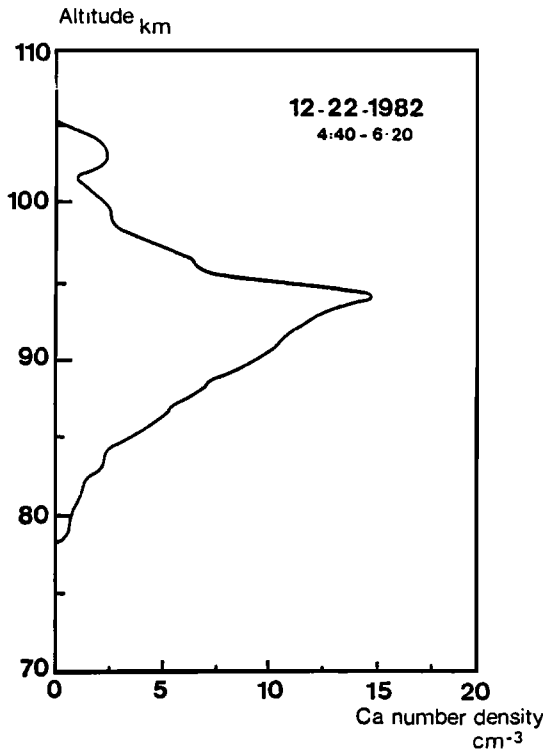


7-15-1983
0:30-1:10

Ca number density cm$^{-3}$

Fig. 2. Calcium atom height profiles obtained by Lidar at the Observatoire de Haute-Provence : a) on December 21/22, 1982, averaged from 4:40 a.m. to 6:20 a.m. b) on July 14/15, 1983, averaged from 0:30 a.m. to 1:10 a.m.

Altitude km



Ca$^+$ number density (cm$^{-3}$)

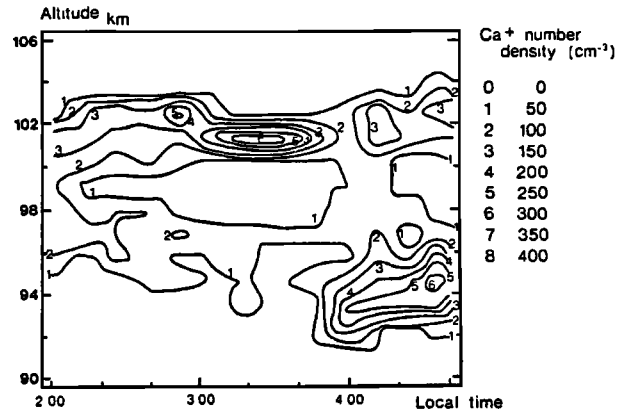| 0 | 0 |
| 1 | 50 |
| 2 | 100 |
| 3 | 150 |
| 4 | 200 |
| 5 | 250 |
| 6 | 300 |
| 7 | 350 |
| 8 | 400 |

Fig. 3. Calcium ion isodensity contours as a function of local time and altitude (on July, 19, 1983, from 2:00 a.m. to 4:40 a.m.). The density scale is stated in cm$^{-3}$ on the right side of the figure.

the totality of the results obtained on sodium and potassium show the clear preponderance of the atomic species over the ionic species (see for instance Aikin et al., 1977 ; Zbinden et al., 1975 ; Narcisi and Bailey, 1965).

Further detections of neutral calcium were achieved in July, 1983. In Figure 2b, the results obtained on July 15 are presented and can be compared to the first results of December. (They are averaged over a 40 mn period of time). The altitude distribution is very different from the one observed in December. The peak concentration is observed at 99 km (32 atoms cm$^{-3}$) in a 2.5 km wide layer, whereas a secondary maximum is observed at 92 km with a peak concentration of 7 atoms cm$^{-3}$ . If the height profile of neutral calcium seems thus highly variable in time, further observations are required for any statistical analysis or detection of possible seasonal variations.

B. Ca$^+$ detection

The first nighttime lidar detection of Ca$^+$ has been performed in July, 1983. On July 19, the observations have been carried out from 2:00 a.m. to 4:40 a.m.. The total abundance as observed during the observation period is larger or equal to 6x10$^7$ ions cm$^{-2}$ and the Ca$^+$ ions are concentrated in thin layers with an average width of 2 to 4 km. Due to the high signal to noise ratio observed, the evolution of the ionic layers have been represented in terms of time height number density isocontours with a temporal resolution of 10 mn and a vertical resolution of 600 m (Figure 3).

From 2:00 a.m. to 3:45 a.m., the layer, at the beginning spread in the 95-105 km altitude range, is getting sharper and centered at an altitude of 101 km. At 3:30 a.m. the width of the Ca$^+$ layer is reduced to 2 km and the mean concentration is 200 ions cm$^{-3}$ . At 3:50 a.m., one notes a drastic change of the peak altitude of the layer from 101 km down to 94 km. From 4:00 a.m. to 4:40 a.m., the vertical profile peaking at 94 km remains essentially stable, but a slight increase of the abundance occurs at the upper altitudes around 102 km. At 4:30 a.m. the

total abundance is $1\times10^8$ ions $cm^{-2}$ for the lower layer and $5\times10^7$ ions $cm^{-2}$ for the upper layer. This latter value of the abundance in the lower layer, $1\times10^8 cm^{-2}$, is larger than the ones generally measured during daytime by rocket borne mass spectrometers at mid latitudes. However the spread in these measurement values is large and an explanation might be found in the great variability of the $Ca^+$ layer as observed during the night of July, 19. The upper $Ca^+$ layer characteristics (peak altitude, abundance of $Ca^+$, thickness) are quite compatible with the presence of a sporadic-E layer. Metallic sporadic-E layer composition is well documented by the mass spectrometer observations and it seems thus likely that the seasonal variation of the $Ca^+$ emission detected in the twilightglow by Broadfoot (1967) could have been related to the occurrence of such layers (high altitude of the layer, summertime occurrence, large abundance) and not to an increase in the background ionized calcium.

## Conclusion

The first nighttime resonant lidar detections of neutral and ionized calcium in the earth's upper atmosphere have brought an unique set of data which seems to confirm the present ideas on the dynamical and chemical behaviour of the metallic atoms and ions (Jégou et al., 1985); furthermore, this has proved the capability of the resonant lidar to follow the evolution of metallic Es layers. From these preliminary measurements, two main results which will however require a further analysis must be retained.

- The changing structure and abundance of the "permanent" $Ca^+$ layer located around the 92 km altitude (until now the layer characteristics were only documented by the mass spectrometer measurements);

- The low abundance in the atomic calcium layer when compared to the sodium abundance, contrasting with an equivalent abundance in the meteoric source.

## References

Aikin, A.C., R.A. Goldberg, W. Jones and J.A. Kane, Observations of mid-latitude lower ionosphere in winter, J. Geophys. Res., 82, 1869-1875, 1977.

Anders, E., and M. Ebihara, Solar system abundances of the elements, Geochim. Cosmochim. Acta, 46, 2363-2380, 1982.

Bos, F., Versatile high-power single-longitudinal-mode pulsed dye laser, Appl. Optics, 20, 1886-1890, 1981.

Broadfoot, A.L., Twilight $Ca^+$ emission from meteor trails up to 280 km, Planet. Space Sci., 15, 503-514, 1967.

Broadfoot, A.L., and A.E. Johanson, Fe (3860

A ) emission in the twilight, J. Geophys. Res., 81, 1331-1334, 1976.

Bucchia, M., and Mégie, G., Ground-based active remote sensing of the night-time stratospheric nitrogen dioxide, Ann. Geophysicae, 1, 411-414, 1983.

Cahen, C., J.P. Jegou, J. Pelon, P. Gildwarg and J. Porteneuve, Wavelength stabilization and control of the emission of pulsed dye lasers by means of a multibeam Fizeau interferometer, Revue Phys. Appl., 16, 353-358, 1981.

Clemesha, B.R., D.M. Simonich, P.P. Batista, and V.W.J.H. Kirchhoff, The diurnal variation of atmospheric Sodium, J. Geophys. Res., 87, 181-186, 1982.

Gadsden, M., Antartic twilight observations-1-Search for metallic emission lines, Ann. Geophys., 25, 667-677, 1969.

Granier, C., and G. Mégie, Daytime Lidar measurements of the mesospheric sodium layer, Planet. Space Science., 30, 169-177, 1982.

Jégou, J.P., M.L. Chanin, G. Mégie and J.E. Blamont, Lidar measurements of atmospheric Lithium, Geophys. Res. Lett., 7, 995-998, 1980.

Jégou, J.P., C. Granier, M.L. Chanin and G. Mégie, General theory of the alkali metals present in the Earth's upper atmosphere. I. Flux model : chemical and dynamical processes, Annales Geophysicae, 3, 163-176, 1985.

Mégie G., F. Bos, J.E. Blamont and M.L. Chanin, Simultaneous nighttime lidar measurements of atmospheric Sodium and Potassium, Planet. Space Sci., 26, 27-35, 1978.

Narcisi, R.S. and A.D. Bailey, Mass spectrometric measurements of positive ions at altitudes from 64 to 112 kilometers, J. Geophys. Res., 70, 3687-3700, 1965.

Richter, E.S., Sechrist Jr., C.F. A meteor ablation-cluster ion atmospheric sodium theory, Geophys. Res. Lett., 6, 183-186, 1979.

Shelton, J.D., C.S. Gardner and C.F. Sechrist, Jr., Density response of the mesospheric Sodium layer to gravity wave perturbations, Geophys. Res. Lett., 7, 1069-1072, 1980.

U.S. Standard Atmosphere, 1976.

Tepley, C.A., J.D. Mathews, J.W. Merimether, Jr., and J.C.G. Walker, Observations of the $Ca^+$ twilight airglow from intermediate layers of ionization, J. Geophys. Res., 86, 7781-7786, 1981.

Zbinden, P.A., M.A. Hidalgo, P. Eberhardt, and J. Geiss, Mass spectrometer measurements of the positive ion composition in the D and E regions of the ionosphere, Planet. Space Sci., 23, 1621-1642, 1975.

C. Granier, J.P. Jegou and G. Mégie, Service d'Aéronomie du CNRS, B.P.3, 91370 - Verrières le Buisson - France